J. Fluid Mech. (1985), *vol.* 150, *pp.* 381–394
Printed in Great Britain

Couette flow of two fluids between concentric cylinders

By YURIKO RENARDY

Mathematics Research Center, University of Wisconsin–Madison,
610 Walnut Street, Madison WI 53705

AND DANIEL D. JOSEPH

Department of Aerospace Engineering, 107 Akerman Hall,
110 Union Street S.E., University of Minnesota, MN 55455

(Received 30 November 1983 and in revised form 7 August 1984)

We consider the flow of two immiscible fluids lying between concentric cylinders when the outer cylinder is fixed and the inner one rotates. The interface is assumed to be concentric with the cylinders, and gravitational effects are neglected. We present a numerical study of the effect of different viscosities, different densities and surface tension on the linear stability of the Couette flow. Our results indicate that, with surface tension, a thin layer of the less-viscous fluid next to either cylinder is linearly stable and that it is possible to have stability with the less dense fluid lying outside. The stable configuration with the less-viscous fluid next to the inner cylinder is more stable than the one with the less-viscous fluid next to the outer cylinder. The onset of Taylor instability for one-fluid flow may be delayed by the addition of a thin layer of less-viscous fluid on the inner wall and promoted by a thin layer of more-viscous fluid on the inner wall.

1. Introduction

We consider linear stability of the flow of two immiscible fluids separated by an interface, lying between concentric rotating cylinders. In each fluid, the Navier–Stokes equations for steady flow are assumed to hold. If we prescribe the ratio of the total volume occupied by each fluid, then the interface is an unknown, across which the velocity and normal and shear stresses are to be continuous. If the fluids have equal or nearly equal densities, then a continuum of interface positions are allowed (Joseph, Renardy & Renardy 1984). However, this non-uniqueness is not borne out by the experiments of Joseph, Nguyen & Beavers (1984), hereinafter referred to as JNB. They use water and various oils as the two fluids in an apparatus with the outer cylinder fixed (see figures 26–30, JNB). When the inner cylinder is rotated at even moderate speeds, gravity effects appear negligible and a pattern consisting of two types of cells is usually observed. One type consists mostly of oil rollers stuck to the inner cylinder and rotating almost like a solid body, lubricated by a thin layer of water at the outer cylinder. The second type consists mainly of water cells undergoing Taylor-vortex motions. These cells extend from the inner to the outer cylinder, but, in some experiments, are covered by a thin layer of oil at the outer cylinder. The two types of cells alternate along the length of the cylinder. This flow is one of many steady bicomponent flows where a study of the selection mechanism for the arrangement of the fluids must be made. At the same time, systematic experiments must be performed since the experiments of JNB are not sufficiently

quantitative to allow a direct comparison with the theory presented here. However, some qualitative features of their experimental results are correlated with our results of §4. One correlation is the thin lubrication layer of water described above. The stability of this arrangement is consistent with our calculations which indicate that we may observe a very thin layer of the less viscous fluid lying next to either the inner or the outer cylinder. Another correlation is the observation of the water cells covered at the outer cylinder by a layer of oil, as illustrated in Fig. 31(c) of JNB. In this arrangement the denser fluid lies next to the inner cylinder whereas intuition suggests that the denser fluid should be the outer fluid. An explanation is required as to why this adverse density difference is observed, and to this end we present a theoretical situation in §4 where an arrangement with an adverse density difference is stabilized by a combination of surface tension and a favourable viscosity difference.

One way to study selection is to study stability, and in this paper we study stability by computing eigenvalues for the spectral problem associated with the linear theory. The equations for our numerical computations are given in §2. Some asymptotic results for short waves are presented in §3, following the ideas of Hooper & Boyd (1983). They consider unbounded Couette flow, but their method of analysis applies locally at any interface with a viscosity jump. Hooper & Boyd showed that in the absence of surface tension the flow is unstable to sufficiently short waves which have wave vectors parallel to the basic flow. The growth rates of these disturbances, however, tend to zero as the waves get shorter. They found that these short-wave instabilities are not suppressed by viscosity as they are in one-fluid flows, but by surface tension. A density difference can stabilize or destabilize them, but not as effectively as surface tension. In §3 we have given a similar analysis for disturbances whose wave vectors are perpendicular to the basic flow. Our results include surface tension, density difference and centrifugal effects. We have correlated our numerical results with the asymptotic formulas.

When surface tension is effective, the longer waves can cause instability, and, if periodic boundary conditions are imposed, then this yields a familiar type of instability in which the interaction of a finite number of modes determines what type of solutions bifurcate from the unstable one (Renardy & Joseph 1984). However, when surface tension is not effective, then we have an unusual instability in which the flow is unstable to all short waves below a certain critical size. This type of instability may play a role in the formation of emulsions.

In §4 we give numerical results for two situations: low Reynolds numbers and Taylor numbers near a critical value. We find that in the preferred configurations a thin layer of the less-viscous fluid may lie next to either cylinder. Our results contradict the selection principle based on minimizing the viscous dissipation in the restricted class of annular layers of two fluids which do not vary along the axis of the cylinder. The solution of this minimization problem (JNB) consists of the less-viscous fluid lying on the inner cylinder, no matter which cylinder rotates. In fact, our numerical results indicate that a narrow stable layer of the less-viscous fluid on the inner cylinder is 'more' stable than that on the outer cylinder. It is also of interest that the instability leading to Taylor vortices in one-fluid flows may be nullified by adding a lubrication layer of the less-viscous fluid at the inner cylinder and that instability may be created by adding a thin layer of more-viscous fluid at the inner cylinder.

2. Stability equations and numerical solution

We use cylindrical coordinates (r^*, θ, z^*), where the z^* axis is the axis of two concentric cylinders. The inner cylinder has radius R_1 and angular velocity Ω_1. The outer cylinder has radius R_2 and angular velocity Ω_2. We consider the stability of a circular Couette flow of two fluids lying between the cylinders. The unperturbed interface is at radius D. We refer to the fluid occupying $R_1 \leqslant r^* \leqslant D$ as the 'inner' fluid and use subscript 1 for its fluid properties. The fluid occupying $D \leqslant r^* \leqslant R_2$ is referred to as the 'outer' fluid and we use subscript 2 for its properties. The viscosities and densities of the fluids are μ_i and ρ_i for $i = 1, 2$.

We introduce the following dimensionless variables (asterisks here denote dimensional variables):

$$(r, z) = \frac{(r^*, z^*)}{R_1}, \quad t = t^*\Omega_1, \quad \boldsymbol{u} = \frac{\boldsymbol{u}^*}{\Omega_1 R_1}, \quad p = \frac{p^*}{\rho_1 \Omega_1^2 R_1^2}.$$

The unperturbed flow has an azimuthal velocity field given by $V_i(r) = A_i r + B_i/r$, $i = 1, 2$, where

$$A_1 = \left(m\left(\frac{R_1^2}{R_2^2} - \frac{R_1^2}{D^2}\right) + \left(\frac{R_1^2}{D^2} - \frac{\Omega_2}{\Omega_1}\right)\right)\Big/ q,$$

$$B_1 = \left(\frac{\Omega_2}{\Omega_1} - 1\right)\Big/ q,$$

$$A_2 = \left(\left(\frac{R_1^2}{R_2^2} - \frac{\Omega_2}{\Omega_1}\frac{R_1^2}{D^2}\right) + m\frac{\Omega_2}{\Omega_1}\left(\frac{R_1^2}{D^2} - 1\right)\right)\Big/ q,$$

$$B_2 = \left(\frac{\Omega_2}{\Omega_1} - 1\right) m/q,$$

$$q = m\left(\frac{R_1^2}{R_2^2} - \frac{R_1^2}{D^2}\right) + \left(\frac{R_1^2}{D^2} - 1\right),$$

$$m = \mu_1/\mu_2.$$

We superimpose an infinitesimal disturbance

$$(u(r), v(r), w(r); p(r)) \exp(-\mathrm{i}\sigma t + \mathrm{i}\alpha z + \mathrm{i}n\theta)$$

so that in each fluid the Navier–Stokes equations yield

$$\mathrm{i}\left(-\sigma + \frac{Vn}{r}\right) w = -\mathrm{i}\alpha \frac{\rho_1}{\rho} p + \frac{\nu}{\Omega_1 R_1^2}\left(\frac{1}{r}(rw')' - \frac{n^2}{r^2} w - \alpha^2 \omega\right), \tag{1}$$

$$\mathrm{i}\left(-\sigma + \frac{Vn}{r}\right) u - \frac{2Vv}{r} = -\frac{\rho_1}{\rho} p' + \frac{\nu}{\Omega_1 R_1^2}\left(\frac{1}{r}(ru')' - (n^2+1)\frac{u}{r^2} - \alpha^2 u - \frac{2\mathrm{i}nv}{r^2}\right), \tag{2}$$

$$\mathrm{i}\left(-\sigma + \frac{Vn}{r}\right) v + 2Au = -\mathrm{i}n \frac{\rho_1 p}{\rho r} + \frac{\nu}{\Omega_1 R_1^2}\left(\frac{1}{r}(rv')' - (n^2+1)\frac{v}{r^2} - \alpha^2 v + \frac{2\mathrm{i}nu}{r^2}\right), \tag{3}$$

where $\nu = \mu/\rho$. Primes denote differentiation with respect to r. Incompressibility yields

$$(ru)' + \mathrm{i}nv + \mathrm{i}r\alpha w = 0. \tag{4}$$

The flat interface $r = D/R_1$ is also perturbed with the factor $\exp(-\mathrm{i}\sigma t + \mathrm{i}\alpha z + \mathrm{i}n\theta)$, and the following linearized conditions hold at $r = D/R_1$ (see Joseph *et al.* 1985). $[\![\ ]\!]$ denotes the difference $(\ )_1 - (\ )_2$ across $r = D/R_1$.

(i) Continuity of velocity:

$$[\![u]\!] = 0, \quad [\![w]\!] = 0,$$

$$\mathrm{i}\left(-\sigma + Vn\frac{R_1}{D}\right)[\![v]\!] = 2u[\![B]\!]\frac{R_1^2}{D^2}.$$

(ii) Continuity of shear stresses and balance of normal stress by surface tension:

$$\mathrm{i}\alpha u[\![\mu]\!] + [\![w'\mu]\!] = 0,$$

$$\left[\!\!\left[\mu\left(\frac{v}{r}\right)'\right]\!\!\right] + \mathrm{i}nu\frac{R_1^2}{D^2}[\![\mu]\!] = 0,$$

$$\mathrm{i}\left(-\sigma + Vn\frac{R_1}{D}\right)\left([\![p]\!] - \frac{2}{\rho_1 \Omega_1 R_1^2}[\![\mu u']\!]\right) + u\frac{R_1 V^2}{D\rho_1}[\![\rho]\!] - \frac{Su}{\rho_1 \Omega_1^2 R_1^3}\left((n^2-1)\frac{R_1^2}{D^2} + \alpha^2\right) = 0,$$

where S is the surface tension and V denotes the basic velocity at the unperturbed interface. Boundary conditions at the solids are

$$u = 0, \quad v = 0, \quad w = 0 \quad \text{at } r = 1, R_2/R_1.$$

We now describe our discretization scheme. Equations (1) and (4) are used to eliminate w and p from (2) and (3). A Chebyschev-polynomial expansion (Orszag 1971) is used for u, v, w and p. If $n+1$ and n Chebyschev polynomials are used for u and v respectively, then the total number of unknowns is $4n+2$. Equation (2) can then be truncated after the $(n-4)$th degree because of the presence of $r^4 u^{\mathrm{iv}}$ and $r^3 v'''$. Equation (3) should be truncated after the $(n-3)$th degree because of the presence of $r^3 u'''$ and $r^2 v''$. The resulting system of linear equations for σ were solved with an IMSL routine on a VAX/VMS 11/780 in complex double precision. The computations were checked against table 2 of Krueger, Gross & DiPrima (1966), Hooper & Boyd's asymptotics for large n and the asymptotics in §3 for large α.

When the two fluids are identical, the presence of the interface introduces a neutrally stable eigenvalue for each n and α (called the 'interfacial' eigenvalue by Yih 1967) in addition to the eigenvalues for one-fluid flow (called 'Taylor' eigenvalues in §4). In §4 we track the behaviour of the interfacial and Taylor eigenvalues as the viscosities, densities, surface tension and volume ratio are changed.

3. Asymptotic analysis for short-wave disturbances

Hooper & Boyd (1983) restrict their asymptotic analysis to two dimensions with coordinates (x, y), where x is the direction of the stream. They consider disturbances in normal modes proportional to $\exp(\mathrm{i}\alpha x)$ for large α or short waves, and expand the stream function and the interfacial eigenvalue in powers of $1/\alpha^2$. The perturbation problems which arise from this procedure are uniquely solvable. Since our stream is in the azimuthal direction, we must replace α by n. The results of Hooper & Boyd apply when n is large and centrifugal effects are neglected. Centrifugal effects considered here, however, play the same role as gravity in their analysis. (We note that a factor α should multiply the gravity term below (16) in their paper.) For large n we find that

$$\sigma \sim nV\left(\frac{D}{R_1}\right)\frac{R_1}{D} + \mathrm{i}\left(2B_1\frac{R_1}{D}\right)^2 \frac{\Omega_1 R_1^2}{\nu_1}\frac{m}{2n^2(1+m)}\left(f - \frac{(1-m)}{(1+m)}\left(\frac{m^2}{\gamma} - 1\right)\right), \tag{5}$$

where
$$f = \frac{nF(\gamma-1)}{bm} - \left(\frac{n}{b}\right)^3 K,$$
$$b = \left(2B_1 \frac{\Omega_1 R_1^2}{\nu_1}\right)^{\frac{1}{2}}, \quad F = \frac{V^2(D/R_1)\,\Omega_1 D^2}{2bB_1 \nu_2},$$
$$K = \frac{DbS}{2B_1 \mu_1 \Omega_1 R_1^2}, \quad \gamma = \frac{\rho_1}{\rho_2}.$$

The parameter F measures the centrifugal force and K is a surface-tension parameter. The parameter f contains the terms in the expression for the growth rate (Im (σ)) that depend on n. We note that this formula was obtained by taking a distinguished limit assuming that the term f remains of order 1 for large n. Hence if either nF or n^3K becomes large the dominant terms in (5) yield the asymptotic behaviour, but the remaining terms in (5) cannot be interpreted as the correction terms of lower order in n. Moreover, if surface tension is not zero the term n^3K eventually dominates the asymptotic formula when n is large enough so that it effectively suppresses short waves.

We can also do short-wave asymptotics for disturbances perpendicular to the (r, θ)-plane. We consider axisymmetric $(n = 0)$ disturbances and introduce the following dimensionless variables:
$$R = \frac{\alpha_1 b(r^* - D)}{D}, \quad T = \frac{2B_1 t^* \Omega_1 R_1^2}{D^2}, \quad Z = \frac{bz^*}{D}.$$

Assuming now that the disturbance is proportional to $\exp(\mathrm{i}\alpha_1 CT + \mathrm{i}\alpha_1 Z)$, this transformation yields the following six conditions at $R = 0$ as $\alpha_1 \to \infty$:
$$[\![u]\!] = 0, \tag{6}$$
$$\left[\!\left[\frac{\partial u}{\partial R}\right]\!\right] = 0, \tag{7}$$
$$-\mathrm{i}\alpha_1 C[\![v]\!] = u(1-m), \tag{8}$$
$$[\![\mu]\!]\, u + \left[\!\left[\mu \frac{\partial^2 u}{\partial R^2}\right]\!\right] = 0, \tag{9}$$
$$\left[\!\left[\mu \frac{\partial v}{\partial R}\right]\!\right] = 0, \tag{10}$$
$$\left[\!\left[\mu\left(\frac{\partial^3 u}{\partial R^3} - 3\frac{\partial u}{\partial R}\right)\right]\!\right] + \frac{\mu_2 \nu_2 mb^2\,((m/\gamma)\,\mathrm{L}^2 u_1 - \mathrm{L}^2 u_2)\bar{f}}{2\Omega_1 R_1 DV(D/R_1)(1-m)} = 0, \tag{11}$$

where
$$\mathrm{L} \equiv \frac{\mathrm{d}^2}{\mathrm{d}R^2} - 1, \quad \bar{f} = \alpha_1 \frac{F(\gamma-1)}{m} - K\alpha_1^3.$$

The equations of motion and continuity with $\mathrm{d}/\mathrm{d}\theta = 0$ are now expanded about $R = 0$ for large α_1, and, as in the analysis of Hooper & Boyd, $u \sim u_0 + u_1/\alpha_1^2 \ldots$, $\alpha_1 C \sim c_0 + c_1/\alpha_1^2 \ldots$, where the zeroth-order velocity satisfies $\mathrm{L}^3 u_0 = 0$ in each fluid. We find that c_1 is determined by u_0, where
$$u_0 = \begin{cases} \mathrm{e}^R(a_0 + a_1 R + a_2 R^2) & \text{for } R < 0, \\ \mathrm{e}^{-R}(b_0 + b_1 R + b_2 R^2) & \text{for } R > 0. \end{cases}$$

To leading order,

$$v \sim \frac{\alpha_1^2 b^2 \nu \, \mathrm{L}^2 u_0}{2V(D/R_1)\, D\Omega_1 R_1}$$

and

$$[\![p]\!] \sim \frac{\alpha_1 2B_1 R_1^2}{\mu_1 D^2}\left[\!\!\left[\mu\left(\frac{\partial^3 u}{\partial R^3} - \frac{\partial u}{\partial R}\right)\right]\!\!\right] + \frac{\mathrm{i}C\nu_1}{\Omega_1 R_1^2}\frac{\partial u}{\partial R}\frac{[\![\rho]\!]}{\rho_1}.$$

Five of the coefficients in u_0 can be found in terms of the sixth by using the interface conditions (6), (7) and (9)–(11). Condition (8) yields $c_0 = 0$ and an equation for c_1:

$$\frac{-\mathrm{i}c_1 b^2 [\![\nu \, \mathrm{L}^2 u_0]\!]}{2V(D/R_1)\, D\Omega_1 R_1} = u_0(1-m). \tag{12}$$

As with the large-n asymptotics, this formula was obtained by assuming that the terms in $\bar{f}$ remain of order 1 for large α_1.

From (12) we find that

$$c_1 = \frac{\mathrm{i}(1-m)}{4(1+m)}\left(\frac{3V(D/R_1)\, D(\gamma-m)\, m}{2B_1 R_1(m+1)\,\gamma} + \frac{2\bar{f}m}{1-m}\right). \tag{13}$$

4. Numerical results

We compute the growth and decay rates $\mathrm{Im}\,(\sigma)$ for the stability of Couette flow of two fluids. We consider two flow regimes. The first, treated in §§4.1 and 4.2, is flow at small Reynolds numbers. Here, if either fluid filled the flow, the one-fluid flow would be linearly stable. The only mode that can become linearly unstable for the two-fluid flow is the interfacial mode. The second, treated in §4.3, is flow at higher Reynolds numbers, where, if the outer fluid filled the flow, the one-fluid flow would be at a critical Taylor number where linear stability is lost. Here, in addition to the interfacial eigenvalues, the eigenvalues associated with the one-fluid flows can become unstable. This type of loss of stability leads to bifurcation and, finally, to the tesselation of stable (highly viscous) and unstable (Taylor cells in the low-viscosity liquid) regions observed in the experiments of JNB. For each flow regime, we determine which arrangement of the components is stable and the volume ratios of the stable configurations.

4.1. *Stability of Couette flow of two fluids for low speeds neglecting surface tension and density difference*

We compute the growth rates for the following range of variables:

$$\frac{\nu_2}{\Omega_1 R_1^2} = 1, \quad \Omega_2 = 0, \quad m = 0.2\text{–}6, \quad \frac{R_2}{R_1} = 2, \quad \gamma = 1, \quad S = 0;$$

α ranges from 0.01 to 50 and n from 0 to 50. From now on we shall call the less-viscous fluid 'thin' and the more-viscous fluid 'thick'. Under these conditions we find that the configuration with a sufficiently thin layer of the less-viscous fluid, situated next to either cylinder, is stable.

The response to long waves (small α and low n) is as follows. The axisymmetric mode becomes insignificant as $\alpha \to 0$, since in that limit there is no disturbance. For $\alpha < 0.1$ and small Reynolds numbers $Re = \Omega_1 R_1^2/\nu$ the growth rate $\mathrm{Im}\,(\sigma)$ is proportional to $\alpha^2 Re$ when $n = 0$ and to Re when $n \neq 0$. The growth rates in this asymptotic range are shown in figures 1 and 2. In figure 1 the thin fluid is situated next to the inner cylinder, and hence the modes displayed are stable ($\mathrm{Im}\,(\sigma) < 0$) if

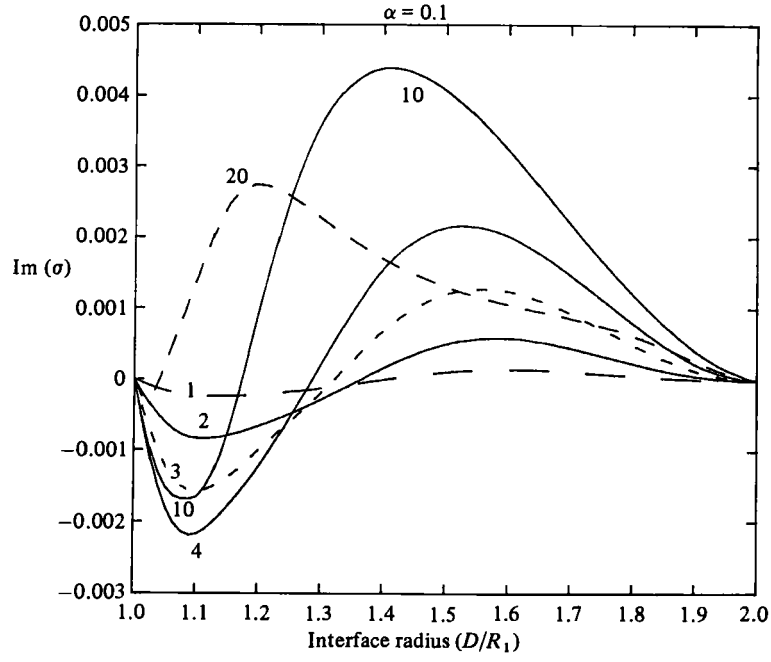

FIGURE 1. Growth rate versus interface position with azimuthal wavenumber n as a parameter. $S = 0$, $\gamma = 1$, $m = 0.4$. The thin fluid is on the inner cylinder. Negative Im (σ) corresponds to stability. When surface tension is absent the flow is unstable at any D ($\neq R_1$ or R_2) if n is large enough. Mode 0 is insignificant under graph scales.

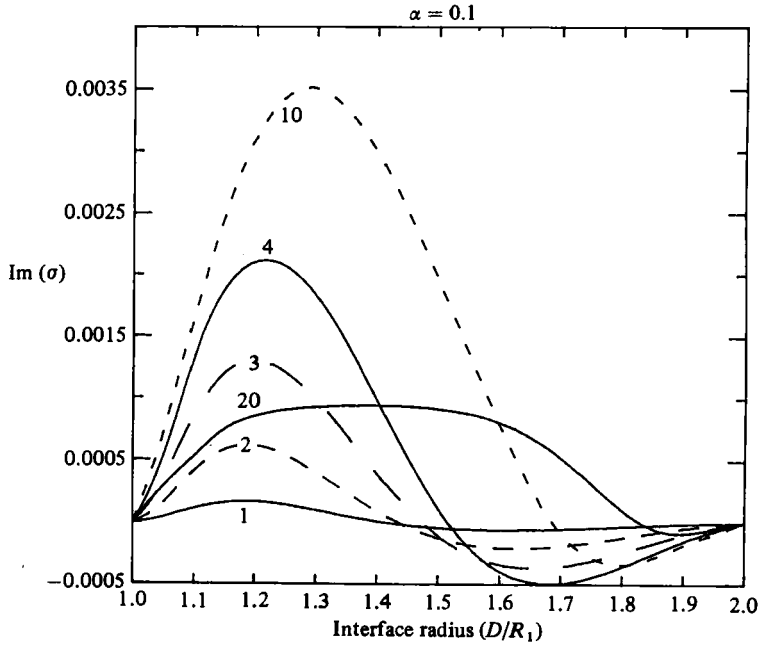

FIGURE 2. Growth rate versus interface position when the thin fluid is on the outer cylinder. $S = 0$, $\gamma = 1$, $m = 2$. The stable modes near the outer cylinder have less stability than the stable modes near the inner cylinder (cf. figure 1) because the decay rates of stable disturbances are much smaller.

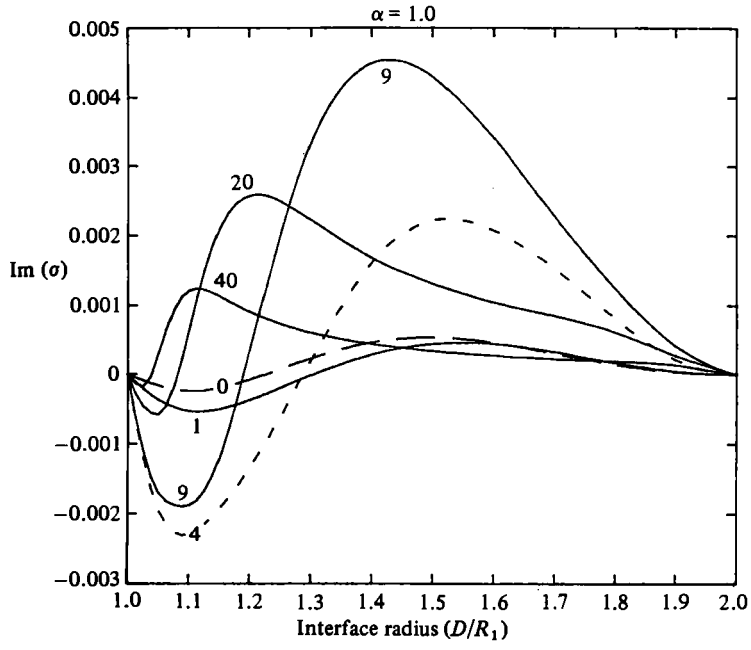

FIGURE 3. Growth-rate curves when the thin fluid is inside. $S = 0$, $\gamma = 1$, $m = 0.4$.

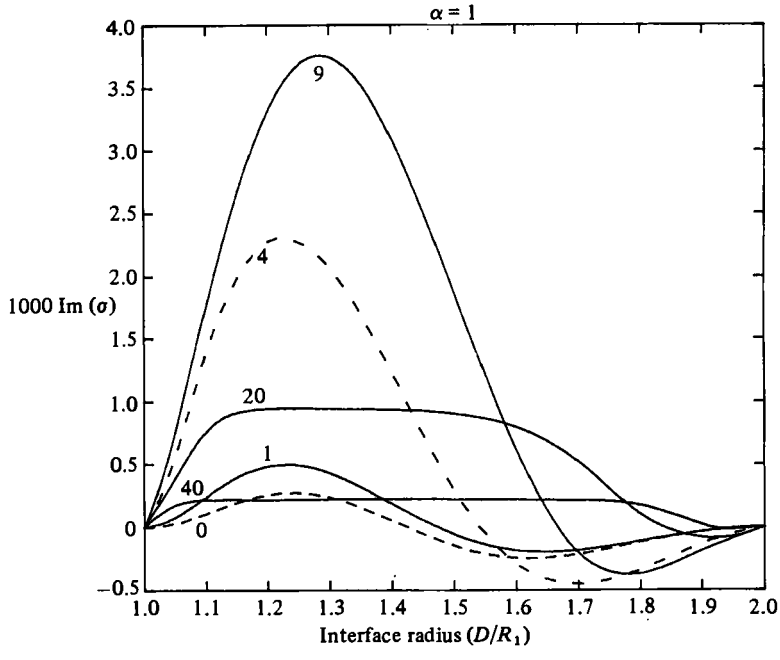

FIGURE 4. Growth-rate curves when the thin fluid is outside. $S = 0$, $\gamma = 1$, $m = 2$. The decay rates of stable disturbances are an order of magnitude smaller than in figure 3.

the interface is close enough to $r = 1$. The situation is reversed in figure 2. In both figures modes 10 and 20 show the short-wave asymptotic behaviour in which the stable range of interface positions, as well as the maximum growth rates, diminish with n (or α). Disturbances of the stable configurations with the thin fluid inside have much larger decay rates than that with thin fluid outside.

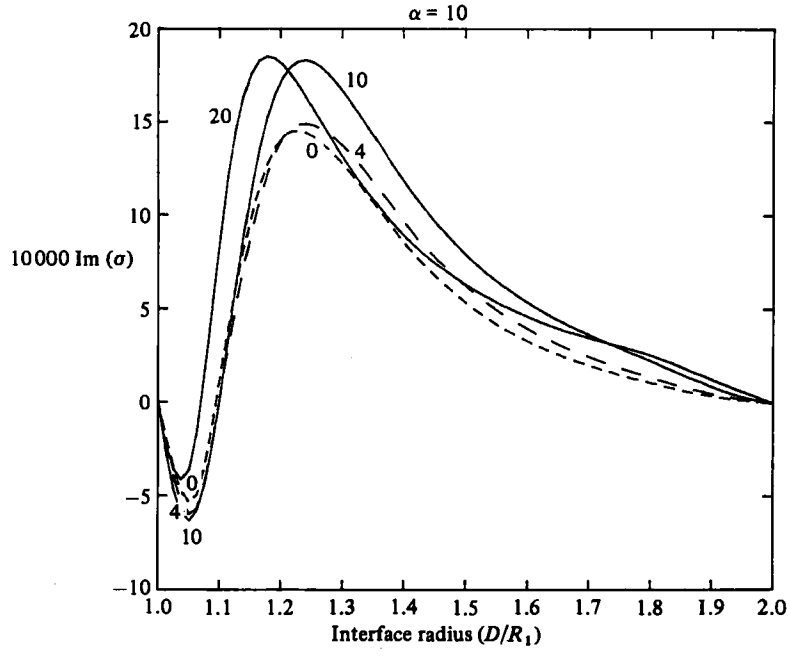

FIGURE 5. Growth rates when the thin fluid is inside. $S = 0$, $\gamma = 1$, $m = 0.4$.

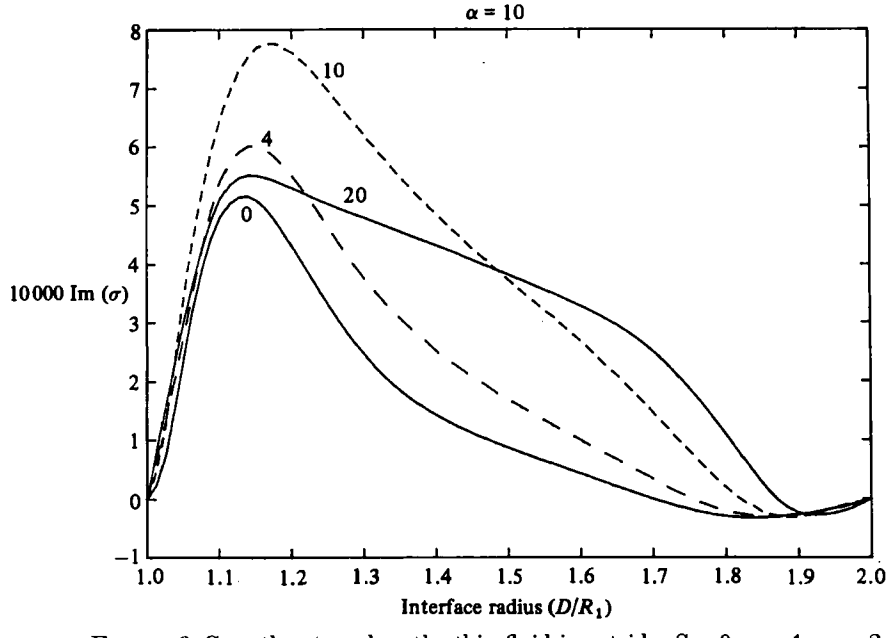

FIGURE 6. Growth rates when the thin fluid is outside. $S = 0$, $\gamma = 1$, $m = 2$.

Trends similar to those exhibited in figures 1 and 2 are exhibited in figures 3 and 4 for $\alpha = 1.0$. The stable range of interface radii is slightly, but not greatly, reduced. Figure 4 clearly shows that for $m = 2$ the dependence of Im (σ) on n at modes 20 and 40 scales with $1/n^2$ over most of the interface positions. In both figures the relative errors of the asymptotic values at $D/R_1 = 1.5$ fall from about 50 % at mode 9 to 8 % at mode 20.

Figures 5 and 6 give growth rates for $\alpha = 10$. For mixed small values of n and large α, (13) yields

$$c_1 \sim \mathrm{i}\frac{3}{8}\frac{(1-m)^2}{(1+m)^2}m^2\left(1-\frac{D^2}{R_2^2}\right), \quad \mathrm{Im}\,(\sigma) \sim \left(\frac{2B_1R_1^2}{D^2}\right)^2\frac{c_1}{\alpha^2}\frac{\Omega_1 R_1^2}{\nu_1}+O(\alpha^{-4}).$$

In figures 5 and 6 modes $n = 1$–3 lie in between modes 0 and 4, and the growth rates of all the modes between 0 and 4 are numerically close. These figures display some qualitative features of large-α asymptotics, but $\alpha = 10$ is not high enough to be in the short-wave asymptotic range for $m = 0.4$ or 2. In addition, the larger the viscosity difference m, the lower is the value of α at which this asymptotic range is attained. For example, at $m = 6$ the relative errors range from 30 % at $\alpha = 10$, 16 % at $\alpha = 20$ and 8 % at $\alpha = 40$, whereas at $m = 2$ (figure 6) these errors are doubled, and at $m = 0.4$ (figure 5) they are quadrupled. As noted by Hooper & Boyd, the short-wave asymptotics break down when the interface is too close to either cylinder.

From our computations, we conclude that the largest growth and decay rates arise in the order-one range of α for medium n and for small m. For example, mode 9 at $\alpha = 1, m = 0.2$ attains three times the growth rate attained at $m = 0.4$ (figure 3), and, in turn, that mode at $m = 0.4$ attains a larger magnitude than at $m = 2$ (figure 4). We may also conclude from a comparison of decay rates that the stable flows with thin fluid inside are 'more' stable than those with thin fluid outside.

4.2. *Stability of Couette flow of two fluids for low speeds: the influence of surface tension and density differences*

Surface tension stabilizes short-wave interfacial disturbances and destabilizes longer waves. Centrifugal forces, in the absence of surface tension, will produce stability if the more-dense fluid is outside. However, with surface tension, it is possible to achieve stability when the denser fluid is inside. This can, of course, only happen if the centrifugal force is not too large and gravity is neglected. Under these conditions, if surface tension is large enough to stabilize the short waves but not so large that the long waves are unstable, then stability is possible at all α and n with the denser fluid inside. One example is $\gamma = 2, m = 2, D/R_1 = 1.9, \nu_2/\Omega_1 R_1^2 = 1, F = 0.00034745$, and $K = 0.592$. Figure 7 shows a graph of $-\mathrm{Im}\,(\sigma)$ versus α, showing stability. Figure 8 shows a graph of $\mathrm{Im}\,(\sigma)$ versus α at zero surface tension, showing that modes become unstable for large α.

4.3. *Stability of Couette flow of two fluids near a critical Taylor number: zero surface tension and density difference*

We recall some properties of the classical Taylor problem for one fluid for which a Taylor number is defined as

$$T_a = 4A\Omega_1(R_2-R_1)^4/\nu,$$

where $A = (\Omega_1 R_1^2-\Omega_2 R_2^2)/(R_1^2-R_2^2)$. For low T_a the flow is linearly stable. As T_a is increased, the first mode to become unstable is the axisymmetric mode $n = 0$. As T_a is increased further the higher modes ($n > 0$) successively become unstable. In this subsection we study the onset of instability for two-fluid flows by fixing properties of the outer fluid so that the axisymmetric mode is at criticality if the entire flow is occupied by that fluid (i.e. $D/R_1 = 1$). We focus on the effect of viscosity stratification and neglect surface tension and density difference effects. Krueger *et al.* (1966) calculated a critical Taylor number for one-fluid flow with the outer cylinder fixed as satisfying $T_a(R_1/R_2)^2 = 1549.59$ and $\alpha = 3.16R_1$. Thus, in our calcula-

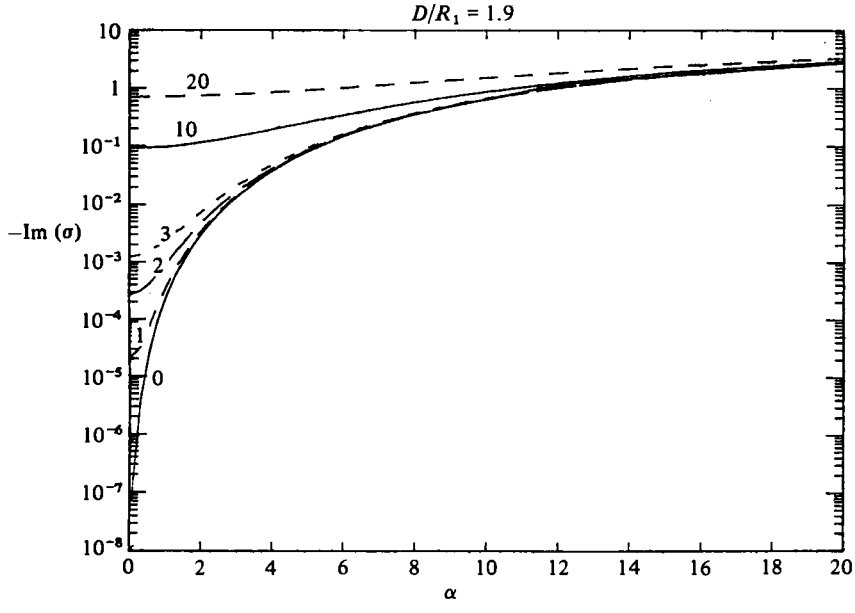

FIGURE 7. Decay rates for the situation with the more-dense fluid in the inner region. $K = 0.592$, $F = 0.00034745$, $\gamma = 2$, $m = 2$. All modes are stable.

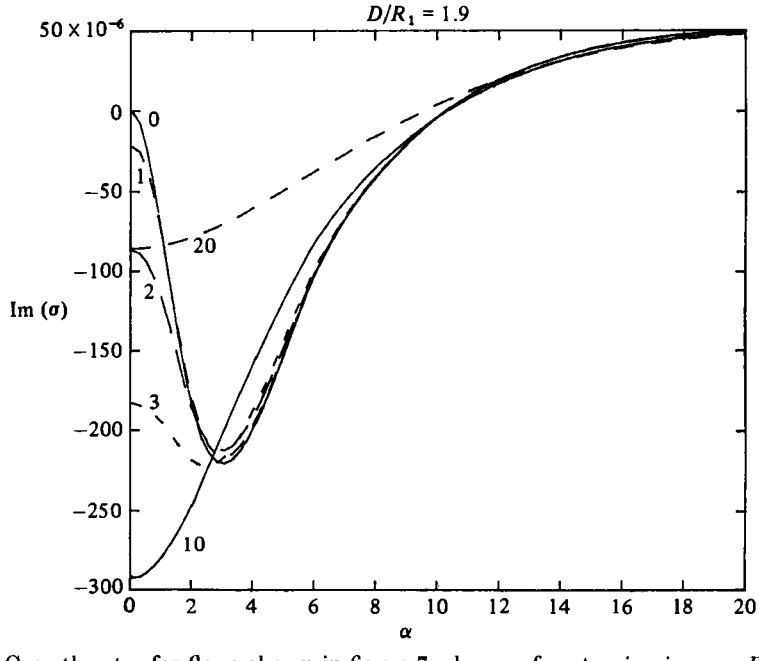

FIGURE 8. Growth rates for flows shown in figure 7 when surface tension is zero. $F = 00034745$, $K = 0$, $\gamma = 2$, $m = 2$. All modes are unstable to sufficiently small (large-α) disturbances.

tions, we set $R_2/R_1 = 2$, $\alpha = 3.16$ and $\nu_2/\Omega_1 R_1^2 = 0.0146$, so that $\mathrm{Im}\,(\sigma)$ for the axisymmetric mode is zero when $D/R_1 = 1$. In each of figures 9–12 the viscosity ratio m is different, and we study the growth rate as the interface position is varied.

We consider two situations: with the thin fluid at the outer ($m > 1$, figures 9 and 10) or at the inner ($m < 1$, figures 11 and 12) cylinder. Intuition would suggest

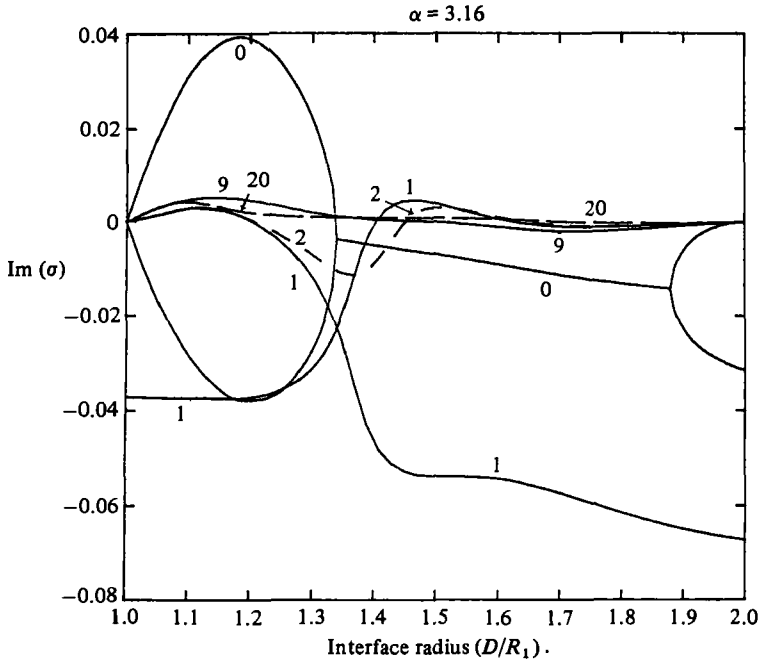

FIGURE 9. Growth rates when the thin fluid lies next to the outer cylinder. $S = 0$, $\gamma = 1$, $m = 1.08$. The amount of thin fluid decreases as D increases but various modes are unstable except when most of the gap is occupied by the thick fluid. At $D/R_1 = 1$ mode 0 is at a critical Taylor number and mode 1 is slightly below.

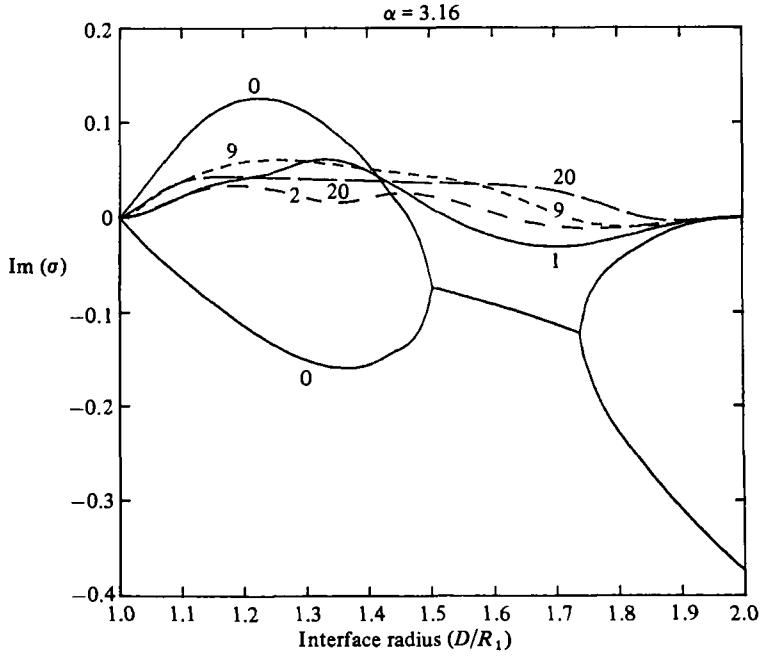

FIGURE 10. Growth rates when the thin fluid is outside. $S = 0$, $\gamma = 1$, $m = 2$. The flow is stable when the thick fluid fills the annulus ($D/R_1 = R_2/R_1 = 2$) and is at criticality when thin fluid fills it ($D/R_1 = 1$). However, the addition of thick fluid at the inner cylinder can actually destabilize the flow unless the thick fluid occupies most of the annulus.

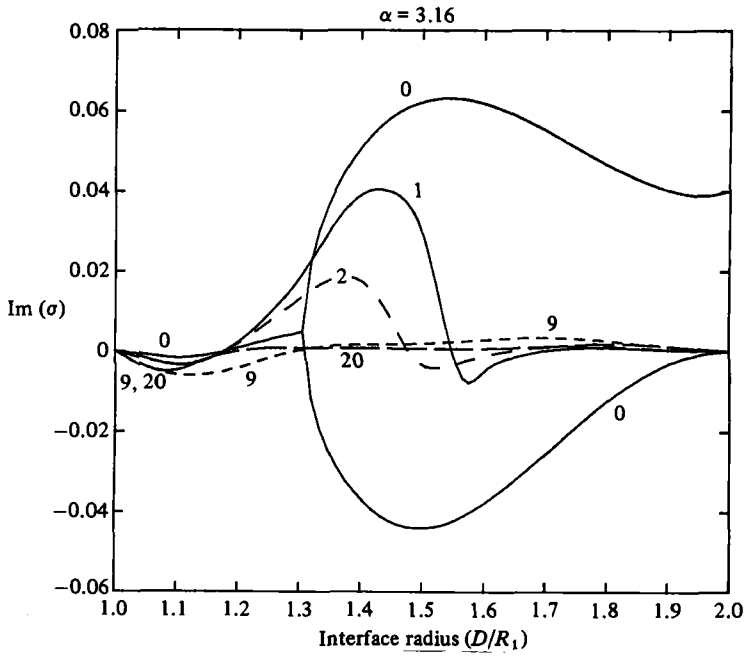

FIGURE 11. Growth rates for various modes when the parameters are close to critical for Taylor instability. $S = 0$, $\gamma = 1$, $m = 0.9$. Thick fluid lies next to the outer cylinder. The addition of thin fluid at the inner cylinder surprisingly stabilizes the flow.

that when $m > 1$ the flow will become more and more stable as D increases because of the presence of increasingly larger amounts of the thick (stable) fluid. This expectation is not realized. Figures 9 and 10 show that various modes become unstable as thick fluid is added. Similarly, intuition would suggest that when $m < 1$ we should have instability for increasing D because more and more thin fluid replaces thick fluid. Figures 11 and 12 show that we actually stabilize the flow by adding thin fluid near the inner wall. This stabilization is associated with the stability of narrow layers and could be called 'lubrication' stabilization associated with the layer of thin fluid on the inner cylinder. In figure 11 mode 0 is unstable if the inner fluid occupies the entire flow. In figure 12 both modes 0 and 1 are unstable if the inner fluid occupies the entire flow.

A new feature close to or above a critical Taylor number is that the Im (σ) for the interfacial eigenvalue need not be single-valued. That is, the graph of Im (σ) versus D/R_1 for an interfacial eigenvalue that begins at $D = R_1$ with Im $(\sigma) = 0$ can proceed to match to a Taylor eigenvalue at $D = R_2$, and a second branch satisfying Im $(\sigma) = 0$ at $D = R_2$ can match to a Taylor eigenvalue at $D = R_1$. Figures 9 and 12 show mode 1 to have such branches. In figure 12 the Taylor eigenvalue for mode 1 is unstable at $D = R_2$, and in figure 9 it is stable at $D = R_2$. The behaviour of the higher $(n > 1)$ modes, for which the Taylor modes are very stable, is as described in §4.1.

For $n = 0$ the equations yield a real-valued problem for $i\sigma, ip, iu, iv$ and iw. Hence $i\sigma$ is either a real number or appears in complex-conjugate pairs. In the latter case the eigenvalues have equal imaginary parts. This behaviour is shown in figures 9–12. For example, in figure 11, for $1 \leqslant D/R_1 \leqslant 1.3$, the $n = 0$ eigenvalues are in conjugate pairs. Near $D/R_1 = 1.3$, Im (σ) splits. One branch becomes increasingly unstable, and at $D = R_2$ is the unstable Taylor eigenvalue for one-fluid flow with $\nu = 0.0132$. The

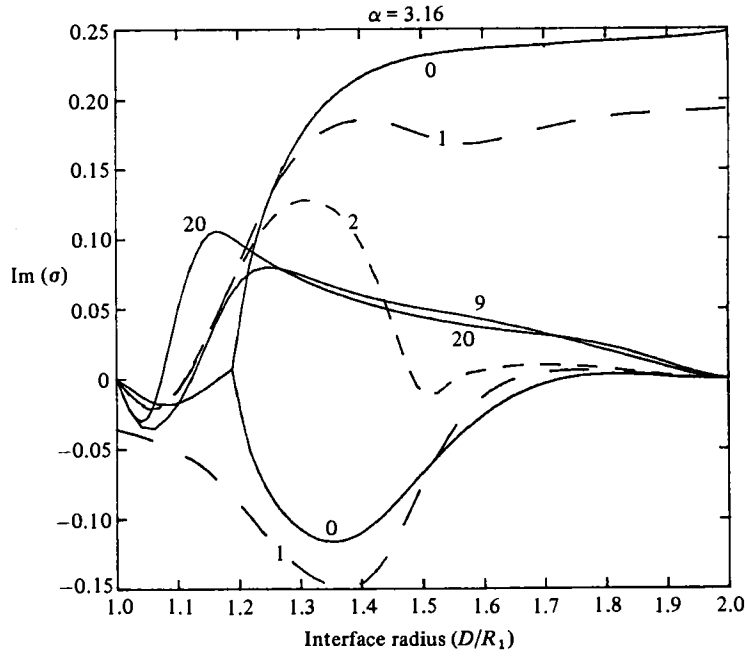

FIGURE 12. Growth rates with thick fluid outside. $S = 0$, $\gamma = 1$, $m = 0.4$. Note the stabilization by a 'lubrication' effect associated with putting a thin layer of less-viscous fluid on the inner cylinder. At $D/R_1 = 1$ mode 0 is at a critical Taylor number and mode 1 is slightly below.

second branch becomes stable for $1.3 \leqslant D/R_1 \leqslant 2$, and, since $\mathrm{Im}\,(\sigma) = 0$ at $D = R_2$, this branch is the interfacial eigenvalue.

Y. Renardy was supported by U.S. Army Contract DAAG 29-80-C-0041. D. Joseph was supported in part by the National Science Foundation and the U.S. Army Research Office.

REFERENCES

HOOPER, A. P. & BOYD, W. G. C. 1983 Shear-flow instability at the interface between two viscous fluids. *J. Fluid Mech.* **128**, 507–528.

JOSEPH, D. D., NGUYEN, K. & BEAVERS, G. S. 1984 Non-uniqueness and stability of the configuration of flow of immiscible fluids with different viscosities. *J. Fluid Mech.* **141**, 319–345.

JOSEPH, D. D., RENARDY, M. & RENARDY, Y. 1984 Instability of the flow of immiscible liquids with different viscosities in a pipe. *J. Fluid Mech.* **141**, 309–317.

JOSEPH, D. D., RENARDY, Y., RENARDY, M. & NGUYEN, K. 1985 Stability of rigid motions and rollers in bicomponent flows of immiscible liquids. *J. Fluid Mech.* (to appear).

KRUEGER, E. R., GROSS, A. & DIPRIMA, R. C. 1966 On the relative importance of Taylor-vortex and non-axisymmetric modes in flow between rotating cylinders. *J. Fluid Mech.* **24**, 521–538.

ORSZAG, S. A. 1971 Accurate solution of the Orr–Sommerfeld stability equation. *J. Fluid Mech.* **50**, 689–703.

RENARDY, M. & JOSEPH, D. D. 1984 Hopf bifurcation in two-component flow. *Maths Res. Center Tech. Summary Rep.* 2689.

YIH, C.-S. 1967 Instability due to viscosity stratification. *J. Fluid Mech.* **27**, 337–352.